Journal of Subsea and Offshore
-Science and Engineering-, Vol.1

March 20, 2015

Wave Induce Motion of Round Shaped FPSO

C. L. Siow,[a,] J. Koto,[a,b,*], H. Yasukawa,[c] A. Matsuda,[d] D. Terada,[d], C. Guedes Soares,[e]
Muhamad Zameri bin Mat Samad,[f] and A.Priyanto,[a]

[a)]*Department of Aeronautics, Automotive and Ocean Engineering, Faculty of Mechanical Engineering, Universiti Teknologi Malaysia*
[b)]*Ocean and Aerospace Research Institute, Indonesia*
[c)]*Department of Transportation and Environmental Systems, Hiroshima University, Japan*
[d)]*National Research Institute of Fisheries Engineering (NRIFE), Japan*
[e)]*Centre for Marine Technology and Engineering (CENTEC), Instituto Superior Técnico, Universidade de Lisboa, Portugal*
[f)]*Department of Materials, Manufacturing and Industrial Engineering, Faculty of Mechanical Engineering, Universiti Teknologi Malaysia*

*Corresponding author: jaswar@mail.fkm.utm.my and jaswar.koto@gmail.com

Paper History

Received: 15-February-2015
Received in revised form: 17-March-2015
Accepted: 19-March-2015

ABSTRACT

Wave response motion and dynamic stability of the new generation Round Shaped FPSO structure in ocean environments is required to be investigated properly to ensure the safety and the operability of this new proposed model. The main objective of this research is to predict the wave induced motion response of the designed Round Shaped FPSO. In this study, the motion response of the Round Shaped FPSO is simulated by diffraction potential theory with Morison heave damping correction method. To ensure the validity of the simulated results, wave tank experiment in the model scale 1:110 was conducted. Upon completed the experiment, the time series data are converted by fast Fourier Transformation method to obtain the response amplitude, RAO of Round Shaped FPSO in 6 degree of freedom measured in the experiment. In the comparison, both the experimental result and numerical result are agreed between each other in this research. Based on the simulation results, it is observed that wave response characteristic and the dynamic stability of the Round Shaped FPSO is good in most of the ocean environment.

KEYWORDS: *Round Shaped FPSO; Wave Response; Diffraction Potential; Damping Correction; Motion Test.*

1.0 INTRODUCTION

Deep water oil and gas exploration is a costly industry activity due to the required of high technology level during exploration. In deep water region, floating structures is more comparative compare to fix structure. Typically, the Floating Production Storage and Offloading, FPSO structure is converted from an old tanker ship but some of the FPSO owner is interest for new constructed hull. In term of system requirement, the FPSO is required better performance in stability either static or dynamic condition compare to resistance performance. The different of operation requirement causes related industry to develop new generation FPSO with more practical hull form to the offshore desire.

In year 2008, Lamport and Josefsson, (2008) carried a research to study the advantage of Round Shaped FPSO over the traditional ship-shaped FPSO [1]. The comparisons were made to compare motion response, mooring system design, constructability and fabrication, operability, safety and costing between both the structures. One of the finding on their study is their designed structures motions are similar for any direction of incident wave with little yaw excitation due to mooring and riser asymmetry. Next, Arslan, Pettersen, and Andersson (2011) are also performed a study on fluid flow around the Round Shaped FPSO in side-by-side offloading condition. FLUENT software was used to simulate three dimensional (3D) unsteady cross flow pass a pair of ship sections in close proximity and the behavior of the vortex-shedding around the two bluff bodies [2].Besides, simulation of fluid flow Characteristic around Round Shaped FPSO by self-develop programming code based on RANs method also conducted by A. Efi et al.[3].

To predict the characteristic of the new Round FPSO concept,

numerical simulation is an effective method to apply in initial study. To study the wave motion response of FPSO, diffraction potential method is frequently used and the accuracy of this method to predict the structures response was also detailed studied. The diffraction potential theory estimates wave exciting forces on the floating body based on the frequency domain and this method can be considered as an efficient one to study the motion of large size floating structure with acceptable accuracy. The good accuracy of this diffraction theory applied to large structures is due to the significant diffraction effect that exists in the large size structure in wave [4].

In this study, the motion response of a Round shaped FPSO is simulated by self-developed programming code based on diffraction potential theory with Morison damping correction method. The accuracy of this programming code is checked with the previous semi-submersible experiment result which carried out at the towing tank belong to Marine Technology Centre, Universiti Teknologi Malaysia [5].

Besides, this research also predicts the wave motion response of this Round shaped FPSO by experimental method. A series of wave tank experiment is conducted at National Research Institute of Fisheries Engineering (NRIFE), Japan. The series of regular wave experimental are conducted with the designed Round FPSO model in scale 1:110. The model also fixed in the wave tank with model scale mooring lines so the experiment can capture the wave frequency motion and slow drifts motion [6]. The mooring design is conducted before the experiment so the suitable mooring line is applied to achieve the experiment target [7]. In this paper, the discussion is focused on the data analysis process and the wave motion response tendency of the designed Round Shaped FPSO.

2.0 NUMERICAL CALCULATION

2.1 Diffraction Potential

In this study, the diffraction potential method was used to obtain the wave force act on the Round Shaped FPSO also the added mass and damping for all six directions of motions. The regular wave acting on floating bodies can be described by velocity potential. The velocity potential normally written in respective to the flow direction and time as below:

$$\Phi(x,y,z) = Re\left[\phi(x,y,z)e^{iwt}\right] \quad (1)$$

$$\phi(x,y,z) = \frac{g\varsigma_a}{iw}\{\phi_0(x,y,z) + \phi_7(x,y,z)\} + \sum_{j=1}^{6} iwX_j\phi_j(x,y,z) \quad (2)$$

where,

g	: Gravity acceleration
ς_a	: Incident wave amplitude
X_j	: Motions amplitude
ϕ_0	: Incident wave potential
ϕ_7	: Scattering wave potential
ϕ_j	: Radiation wave potential due to motions
j	: Direction of motion

From the above equation, it is shown that total wave potential in the system is contributed by the potential of the incident wave, scattering wave and radiation wave. In addition, the phase and amplitude for both the incident wave and scattering wave is assumed to be the same. However, radiation wave potentials are affected by each type of motions of each single floating body inside system, where the total radiation wave potential from the single body is the summation of the radiation wave generates by each type of body motions such as surge, sway, heave, roll, pitch and yaw,

Also, the wave potential $\emptyset$ must be satisfied with boundary conditions as below:

$$\nabla^2\emptyset = 0 \quad for\ 0 \le z \le h \quad (3)$$

$$\frac{\partial\emptyset}{\partial z} + k\emptyset \quad at\ z = 0 \quad \left(k = \frac{w^2}{g}\right) \quad (4)$$

$$\frac{\partial\emptyset}{\partial z} = 0 \quad at\ z = h \quad (5)$$

$$\emptyset \sim \frac{1}{\sqrt{r}}e^{-ik_0 r} \quad should\ be\ 0\ if\ r\ \infty \quad (6)$$

$$\frac{\partial\phi_7}{\partial n} = -\frac{\partial\emptyset_0}{\partial n}\ on\ the\ body\ boundary \quad (7)$$

2.2 Wave Potential

By considering the wave potential only affected by model surface, S_H, the wave potential at any point can be presented by the following equation:

$$\emptyset(P) = \iint_{S_H}\left\{\frac{\partial\emptyset(Q)}{\partial n_Q}G(P;Q) - \emptyset(Q)\frac{\partial G(P;Q)}{\partial n_Q}\right\}dS(Q) \quad (8)$$

Where $P = (x, y, z)$ represents fluid flow pointed at any coordinate and $Q = (\xi, \eta, \varsigma)$ represent any coordinate, (x, y, z) on model surface, S_H. The green function can be applied here to estimate the strength of the wave flow potential. The green function in eq. (8) can be summarized as follow:

$$G(P;Q) = -\frac{1}{4\pi\sqrt{(x-\xi)^2 + (y-\eta)^2 + (z-\zeta)^2}} + H(x-\xi, y-\eta, z+\zeta) \quad (9)$$

Where $H(x-\xi, y-\eta, z+\zeta)$ in eq. (9) represent the effect of free surface and can be solved by second kind of Bessel function.

2.3 Wave Force, Added Mass and Damping

The wave force or moment act on the model to cause the motions of structure can be obtained by integral the diffraction wave potential along the structure surface.

$$E_i = -\iint_{S_H}\phi_D(x,y,z)n_i dS \quad (10)$$

where, ϕ_D is diffraction potential, $\phi_D = \phi_o + \phi_7$

Also, the added mass, A_{ij} and damping, B_{ij} for each motion can be obtained by integral the radiation wave due to each motion along the structure surface.

$$A_{ij} = -\rho\iint_{S_H} Re\left[\phi_j(x,y,z)\right]n_i dS \quad (11)$$

$$B_{ij} = -\rho w \iint_{S_H} Im[\phi_j(x,y,z)]n_i dS \quad (12)$$

Where n_i in eq. (10) to eq. (12) is the normal vector for each direction of motion, i = 1~ 6 represent the direction of motion and j = 1~6 represent the six type of motions

2.4 Drag Term of Morison Equation

The linear drag term due to the wave effect on submerge model is calculated using Drag force equation as given by Morison equation:

$$F_D = \frac{1}{2}\rho A_{Proj} C_D |\dot{\phi}_Z - \dot{X}_z|(\dot{\phi}_Z - \dot{X}_z) \quad (13)$$

Where ρ is fluid density, A_{Proj} is projected area in Z direction, C_D is drag coefficient in wave particular motion direction, $\dot{\phi}_Z$ is velocity of particle motion at Z-direction in complex form and $\dot{X}_z$ is structure velocity at Z-direction

In order to simplify the calculation, the calculation is carried out based on the absolute velocity approach. The floating model dominates term is ignored in the calculation because it is assumed that the fluid particular velocity is much higher compared to structure velocity. Expansion of the equation (13) is shown as follows:

$$F_D = \frac{1}{2}\rho A_{Proj} C_D |\dot{\phi}_Z|(\dot{\phi}_Z) - \frac{1}{2}\rho A_{Proj} C_D |\dot{\phi}_Z|\dot{X}_z - \frac{1}{2}\rho A_{Proj} C_D |\dot{X}_z|\dot{\phi}_Z + \frac{1}{2}\rho A_{Proj} C_D |\dot{X}_z|\dot{X}_z \quad (14)$$

By ignoring all the term consist of $|\dot{X}_z|$, equation (14) can be reduced into following format.

$$F_D = \frac{1}{2}\rho A_{Proj} C_D |\dot{\phi}_Z|(\dot{\phi}_Z) - \frac{1}{2}\rho A_{Proj} C_D |\dot{\phi}_Z|\dot{X}_z \quad (15)$$

The above equation (15) is still highly nonlinear and this is impossible to combine with the linear analysis based on diffraction potential theory. To able the drag force to join with the diffraction force calculated with diffraction potential theory, the nonlinear drag term is then expanded in Fourier series. By using the Fourier series linearization method, equation (15) can be written in the linear form as follow:

$$F_D = \frac{1}{2}\rho A_{Proj} C_D \frac{8}{3\pi} V_{max}(\dot{\phi}_Z) - \frac{1}{2}\rho A_{Proj} C_D \frac{8}{3\pi} V_{max}\dot{X}_z \quad (16)$$

Where, V_{max} in equation (16) is the magnitude of complex fluid particle velocity in Z direction. From the equation (16), it can summarize that the first term is linearize drag force due to wave and the second term is the viscous damping force due to the drag effect.

According to Christina Sjöbris, the linearize term $\frac{8}{3\pi}V_{max}$ in the equation (16) is the standard result which can be obtained if the work of floating structure performance at resonance is assumed equal between nonlinear and linearized damping term [8].

The linearize drag equation as shown in equation (16) now can be combined with the diffraction term which calculated by diffraction potential theory. The modified motion equation is shown as follows:

$$(m + m_a)\ddot{X}_z + \left(b_p + \frac{1}{2}\rho A_{Proj} C_D \frac{8}{3\pi} V_{max}\right)\dot{X}_z + kx = F_p + \frac{1}{2}\rho A_{Proj} C_D \frac{8}{3\pi} V_{max}(\dot{\phi}_Z) \quad (17)$$

Where m is mass, k is restoring force, m_a, b_p, F_p is heave added mass, heave diffraction damping coefficient and heave diffraction force calculated from diffraction potential method respectively. $\frac{1}{2}\rho A_{Proj} C_D \frac{8}{3\pi} V_{max}$ is the viscous damping and $\frac{1}{2}\rho A_{Proj} C_D \frac{8}{3\pi} V_{max}(\dot{\phi}_Z)$ is the drag force based on drag term of Morison equation.

2.5 Differentiation of Wave Potential for Morison Drag Force

To obtain the drag force contributed to heave motion, the wave particle velocity at heave direction must be obtained first. This water particle motion is proposed to obtain from the linear wave potential equation. From the theoretical, differential of the wave potential motion in Z-direction will give the water particle motion in the Z-direction.

As mentioned, the drag force in Morison equation is in the function of time; therefore, the time and space dependent wave potential in the complex should be used here. The wave potential in Euler form as follows:

$$\phi(x,y,z) = \frac{\varsigma g}{w} e^{-Kz + iKR + i\alpha} \quad (18)$$

The expending for the equation (18) obtained that

$$\phi(x,y,z) = \frac{\varsigma g}{w} e^{-Kz} \cdot [\cos(KR) + i\sin(KR)] \cdot [\cos\alpha + i\sin\alpha] \quad (19)$$

Rearrange the equation (19), the simplify equation as follows

$$\phi(x,y,z) = \frac{\varsigma g}{w} e^{-Kz} \cdot [\cos(KR + \alpha) + i\sin(KR) + \alpha] \quad (20)$$

Differentiate the equation (20) to the Z-direction, the water particle velocity at Z-direction is shown as follows:

$$\phi_Z(x,y,z) = \frac{\varsigma g}{w}(-K)e^{-Kz} \cdot [\cos(KR + \alpha) + i\sin(KR) + \alpha] \quad (21)$$

Since this numerical model is built for deep water condition, hence it can replace the equation by $Kg = w^2$ and the equation (21) is becoming as follow:

$$\phi_Z(x,y,z) = \varsigma w e^{-Kz} \cdot [\cos(KR + \alpha) + i\sin(KR + \alpha)] \quad (22)$$

In the equations (18) to (22), ς is the wave amplitude, g is the gravity acceleration, w is the wave speed, K is wave number, R is the horizontal distance referring to zero coordinate, α is the time dependent variable.

The horizontal distance, R and the time dependent variable, α can be calculated by the following equation

$$R = Kx\cos\beta + Ky\sin\beta \quad (23)$$

$$\alpha = wt + \epsilon \quad (24)$$

In equation (23) and equation (24), the variable β is wave heading angle, ϵ is the leading phase of the wave particle velocity at the Z-direction and t is time.

To calculate the drag forces by using the Morison equation, equation (22) can be modified by following the assumptions below.

First, since the Morison equation is a two dimensional method, therefore the projected area of the Z-direction is all projected at the bottom of structure.

Second, as mentioned in the previous part, this method applies the absolute velocity method and the heave motion of model is considered very small and can be neglected; therefore, the change of displacement in Z-direction is neglected.

From the first and second assumption, the variable z at equation (22) is no effected by time and it is a constant and equal to the draught of the structure. By ignore the time series term, and then the equation (22) can be become as follow:

$$\phi_Z(x,y,z) = \varsigma we^{-Kz}\cdot[\mathrm{Cos}(KR) + i\,\mathrm{Sin}(KR)] \quad (24)$$

2.6 Determination of Drag Coefficient

Typically the drag coefficient can be identified from experimental results for the more accurate study. In this study, the drag coefficient is determined based on empirical data calculated based on section 2.6. In order to be able to calculate the empirical data, the Round Shaped FPSO is assumed as a vertical cylinder. Secondly, the laminar flow condition is applied to calculate the drag damping and drag force based on section 2.3, so it is match with the assumption applied in diffraction potential theory.

3.0 WAVE TANK EXPERIMENT

3.1 Experimental Setup

This experiment is conducted in wave dynamic tank with the length, wide and depth of 60m, 25m and 3.2m respectively. Before the experiment start, the Round FPSO model was fixed in the middle of tank by four mooring lines which connected between the fairleads located in bottom of FPSO with the anchors which sink into the bottom of tank. Each anchor used in the experiment has the weight of 20kg in air. The view of FPSO model inside wave dynamic tank after installed with mooring lines is showed in Figure 1.

The Round Shaped FPSO model is experienced six degrees of freedom during the experiment. The linear DOF motions of the FPSO models on model size mooring are measured by theodolite camera system. The theodolite camera is able to capture the positions of the reflective optical tracking markers placed on the FPSO model automatically. In this setup, the height of the reflective optical tracking markers is 0.547m above the vertical center of gravity of the Round Shaped FPSO model [6]. The Rotational DOF motions of the FPSO models are measured by gyroscope installed in the center of gravity of the FPSO.

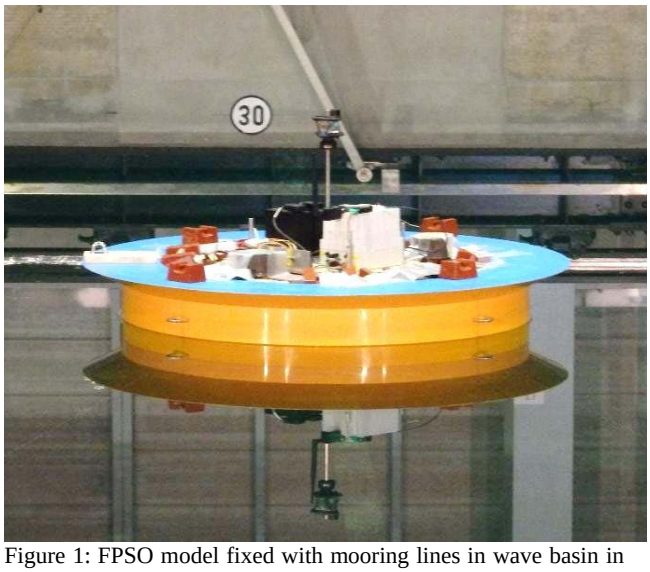

Figure 1: FPSO model fixed with mooring lines in wave basin in static condition.

A servo-type wave height measurement device attached to the carriage which located at the position between FPSO model and wave generator to record the wave height generate by the wave generator. To ensure the wave height measure by wave measuring device is not influence by the existing of Round FPSO, the carriage installed by the servo-type wave height measurement device is moved to the location where the distance between the FPSO to wave measuring device and the distance between wave generator and wave measuring device are 15m both.

All the measurement devices are linked to separate computer to maximize the consistency of the measuring speed. To synchronize the devices and ensure all devices start and stop measure the data without delay, a wireless remove is used to given the order to start and stop all measurement devices [6].

3.2 Linear Motion Data Transformation

As mentioned, the height of the reflective optical tracking markers is 0.547m above the vertical center of gravity of the Round Shaped FPSO model. This also means that the position of the FPSO in wave tank measured by the theodolite camera is not located in the center of gravity of the model. To obtain the exact position of the model referred to model's the center of gravity, the linear motion data must be transferred to the center of gravity of the model. To transfer the data, respective roll, pitch and yaw motion of the model occurred at the same time must be considered in the calculation. The relationships between the positions of the reflective optical tracking markers with the position of center of gravity of model by consider the roll, pitch and yaw motions are showed in Figure 2.

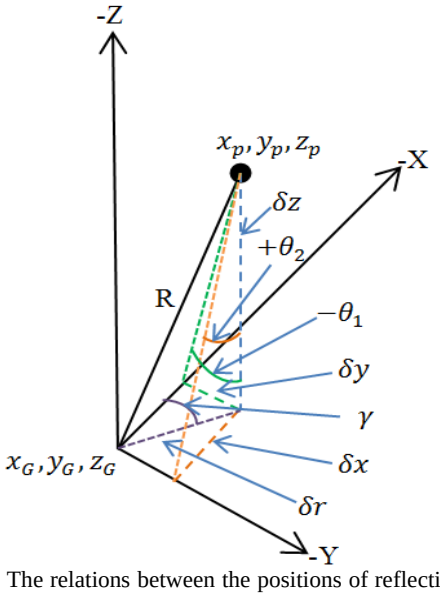

Figure 2: The relations between the positions of reflective optical tracking markers with position of center of gravity of model.

From the Figure 2,x_p, y_p, z_p represent the x, y and z position of the reflective optical tracking markers while x_G, y_G, z_G are the x, y and z position of the center of gravity of model. The relationship between both the position is in the function of length of rod, R, roll angle(θ_1), pitch angle(θ_2), yaw angle (θ_3) and model initial heading angle (γ). Therefore, the position information at model center of gravity can be calculated as follow:

$$x_g = x_p - \delta x \quad (25)$$

$$y_g = y_p - \delta y \quad (26)$$

$$z_g = z_p - R + \delta z \quad (27)$$

Where, $\delta x, \delta y$ and δz can be calculated by following equation

$$\delta z = \left[\frac{R^2}{Tan^2(\theta_1) + Tan^2(\theta_2) + 1}\right]^{1/2} \quad (28)$$

$$\delta r = [R^2 - \delta z^2]^{1/2} \quad (29)$$

$$\alpha = Tan^{-1}\left(\frac{Tan\ \theta_1}{Tan\ \theta_2}\right) \quad (30)$$

$$\delta x = \delta r\ Cos(\theta_3 + \alpha + \gamma) \quad (31)$$

$$\delta y = \delta r\ Sin(\theta_3 + \alpha + \gamma) \quad (32)$$

After the position of model referred to its center of gravity is obtained the for entire time series, the information can be used to calculate all 6 degree of motions of model. In this experiment setup, the Rotational motions of the FPSO models are measured by gyroscope installed in the models' center of gravity, hence, the measured roll, pitch and yaw motion by the gyroscope can be directly used for the model rotational motions data. However, extra treatment is needed for the linear motions which measured by theodolite camera because the time domain position data obtained from the theodolite camera is the model position in the wave tank without consider it direction. By consider the model initial position and initial heading direction, the position data returned from theodolite camera can be used to obtain the model surge, sway and heave motion. In Figure 3, the plan drawing showed the different of global coordinate where these data are measured by theodolite camera and the local coordinate system which required in calculating the linear motion of the FPSO due to the wave.

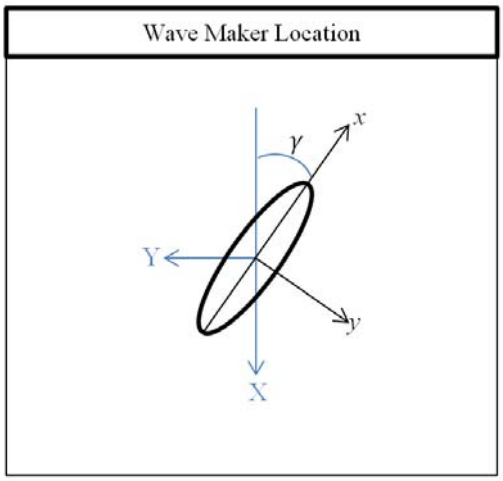

Figure 3: Plan view of coordinate system.

In Figure 3, X and Y represent the global direction use in the experiment setup while *x* and *y* are the local direction where the zero position of local coordinate system is located in the model center of gravity before the wave arrived. The model initial heading angle (γ) is measured from wave progress direction and positive follow clock direction. By reset the zero global coordinates to the model center of gravity at calm sea condition, the 6 DOF motions of the model can be calculated as follow,

$$L = (X^2 + Y^2)^{1/2} \quad (33)$$

$$\beta = Tan^{-1}\frac{Y}{X} \quad (34)$$

And the six degree freedom of motion for the Round Shaped FPSO can be calculated from the equation (35) to equation (40).

$$Surge, E_1 = L\ Cos(\beta - \gamma + 180) \quad (35)$$

$$Sway, E_2 = L\ Sin(\beta - \gamma + 180) \quad (36)$$

$$Heave, E_3 = Z_g \quad (37)$$

$$Roll, E_4 = \theta_1 \quad (38)$$

$$Pitch, E_5 = \theta_2 \quad (39)$$

$$Yaw, E_6 = \theta_3 \quad (40)$$

3.3 Fourier Series Transformation

The experiment data collected in time series provide the information of wave frequency motion for all 6 degree of motion and slow drift motion for horizontal plan motion. To split the different motion data, the analysis can be conducted in frequency domain where the amplitude of the different types of motion can be extracted from the motion amplitude occur at respective frequency.

According to sampling theorem, discretely frequency (Fs) of signal data must be at least twice to the highest continuous signal frequency (F). The continuous signal frequency should discrete by the rate follow the sampling frequency, 1/Fs. Let the discrete sample of the continuous signal have the magnitude of x(k), k=1,2,3,…,n and period between the sample is 1/Fs than a function of a continuous signal, f(t) can be reconstructed back from the discrete sample by the equation below:

$$f(t) = \sum_{k=1}^{k=n} x(k)\, sinc(t \times fs - k) \quad (41)$$

Where,

$$sinc(x) = \frac{\sin(\pi x)}{\pi x} \quad (42)$$

To convert the data in time domain to the frequency domain, Fast Fourier Transform method can be applied. The relationship between function in the time domain, f(t) and frequency domain F(f) can be related by the equation below:

$$F(f) = \int_{-\infty}^{\infty} f(t) e^{-j2\pi f(t)} dt \quad (43)$$

Also, for the variable *j*, it represents the square root of (-1) in the natural exponential function.

$$e^{j\theta} = \cos(\theta) + j \sin(\theta) \quad (44)$$

Therefore, the discrete data can be written in complex number form as follows:

$$x_i = x(i)_{real} + j\, x(i)_{imaginary} \quad (45)$$

And,

$$x(i)_{real} = \sum_{k=0}^{k=n} X(k) \times \cos\left(\frac{2\pi k i}{n}\right) \quad (46)$$

$$x(i)_{imaginert} = \sum_{k=0}^{k=n} X(k) \times \sin\left(\frac{2\pi k i}{n}\right) \quad (47)$$

And, $i = 2^b$ is the number of data require by Fast Fourier Transform method where b can be any integer number larger than or equal to 1.

Finally, the magnitude, phase and frequency of the signal can be calculated by following equations:

$$X(i)_{magnitude} = \|X(i)\| = \frac{2 \times \sqrt{x(i)_{real}{}^2 + x(i)_{imaginert}{}^2}}{n} \quad (48)$$

$$X(i)_{phase} = tan^{-1}\left[\frac{x(i)_{imaginert}}{x(i)_{real}}\right] \quad (49)$$

$$X(i)_{frequency} = i \times \frac{Fs}{n} \quad (50)$$

4.0 MODEL PARTICULARS

The objective of this research is predicting the wave motion response of new designed Round Shaped FPSO. The designed Round Shaped FPSO has the diameter at the draft equal to 111.98meter and draft of 31.91meter. The model was constructed from wood following the scale of 1:110 (Table 1).

Upon the model complete constructed inclining test, and roll decay test were conducted to identify the hydrostatic particular of the Round Shaped FPSO model. The dimension and measured data of the model was summarized as in Table 1.

Table 1:Particular of Round Shaped FPSO

Symbol	Model	Full Scale
Diameter (m)	1.018	111.98
Depth (m)	0.4401	48.41
Draught(m)	0.2901	31.91
Free board(m)	0.150	16.5
Displacement (m^3)	0.2361	314249
Water Plan Area (m^2)	0.8139	9848.5
KG (m	0.2992	32.9
GM (m)	0.069	7.6

In this study, the numerical method is applied to execute the wave motion response of Round Shaped FPSO. The panel method developed based on diffraction potential theory with Morison damping correction as presented at part 2 of this paper required to generate a number of meshes on the model surface in order to predict the distribution of wave force act on this Round FPSO model. To reduce the execution time, symmetry theory is applied in the calculation and total number of panels generated for execution in each symmetry side is525 (1050 for whole model) for immerse part. The sample of mesh of Round Shaped model used in the numerical calculation is shown in Figure 4.

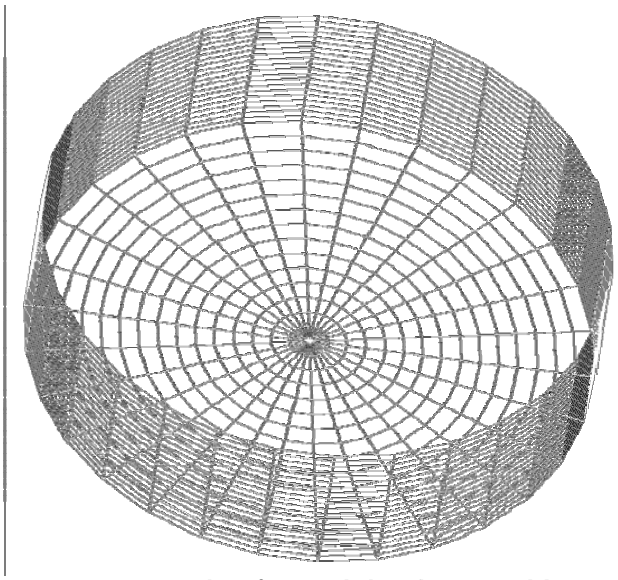

Figure 4: Meshing for Round Shaped FPSO model

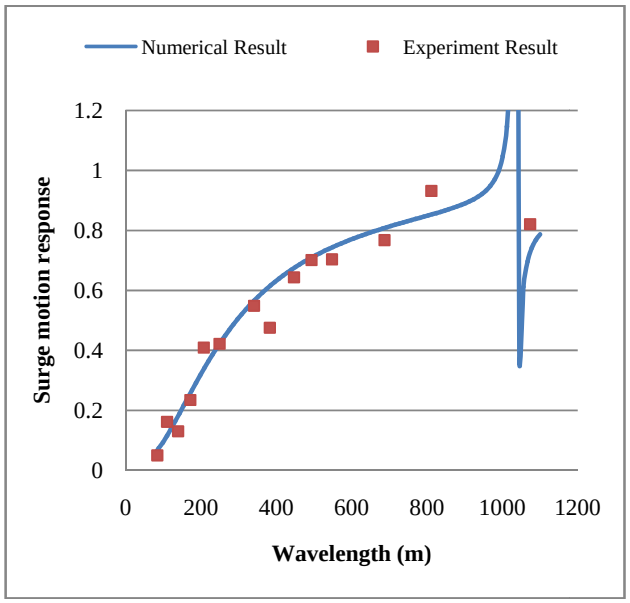

Figure 5: Surge motion responses of Round Shaped FPSO

5.0 RESULT AND DISCUSSION

The numerical result calculated by using diffraction potential theory is compared to experimental result in order to check the accuracy of the simulation result. After that, the discussion is focused in evaluate the wave motion response of the designed Round Shaped FPSO model.

5.1 Numerical and Experimental Simulation

The experiment test is conducted in regular wave condition. In this experiment, the wavelength is proper selected so it can obtain the tendency of all motions response in response to difference wavelength. In this part, the response amplitude of Round Shaped FPSO model in head sea condition was discussed. As shown in Figure 5 to Figure 7, the tendency of surge, pitch and heave motion response obtained by both the numerical and experimental method is agreed between each other.

The numerical result predicted that the surge motion tendency will experience large change of motion response between the wavelengths 900 meter to 1100 meter. However, due to lack of experiment data in this region, the actual condition is difficult to predict.

Besides, the experiment and numerical result also showed that the designed FPSO model will experience large pitch motion at long wave length region as shown in Figure.6. The numerical calculation shows that the pitch response is under estimated at wavelength 400 m. By compare the pitch and surge response tendency calculated by diffraction potential theory, it is showed that the large change of surge tendency at wavelength from 900 meter to 1100 meter may due to the coupling motion of pitch response. The resonance of pitch motion which caused the pitch motion increased significant also influence the surge motion response of this designed model.

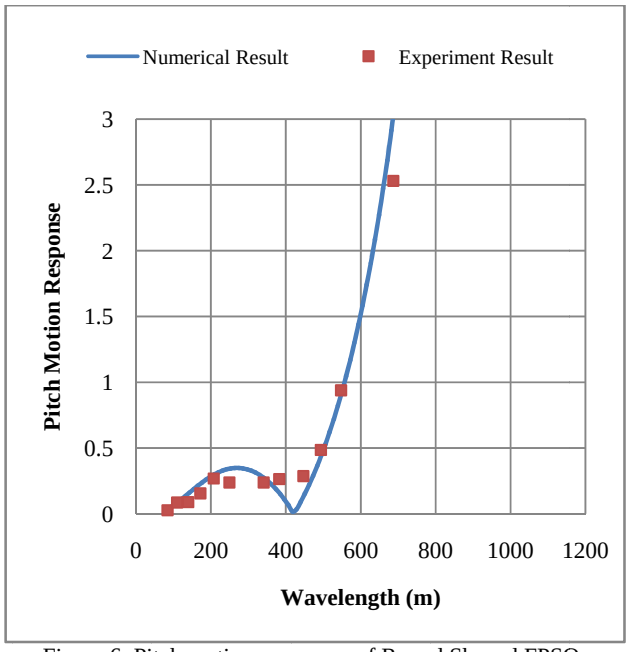

Figure 6: Pitch motion responses of Round Shaped FPSO

Besides, the numerical result also show good agree with experiment result in predicting the heave response tendency. Due to involve the extra viscous damping estimate by the Morison Drag Term in the calculation, the heave response of the Round Shaped FPSO model predict by the numerical method at the damping dominant region did not return a significant over predict error. From the Figure 7, the maximum heave response predicted by the numerical simulation is 1.74 and occurred at wavelength 385meter while the maximum heave response predicted by experiment method is 1.68 and occurred at wavelength 490 meter.

Comparing the heave response tendency predicted by both the methods, the Figure 7 also shown the numerical result (blue line) is fixed quite well to the heave response data collected from experiment (red dot). This shown that the developed numerical method which combined the Morison drag term with diffraction potential theory can be applied to predict the heave response of this Round Shaped FPSO even in damping dominate region and obtained reasonable accuracy result.
In overall, it can observed that the numerical result is able to predict the 6 DOF wave motion response of the Round Shaped FPSO in good accuracy if compare to experiment result. Since this designed FPSO model is 4 side symmetry (bow and stern, port-side and starboard side), then the study conducted in the head sea condition is enough to present the motion response characteristic of this model.

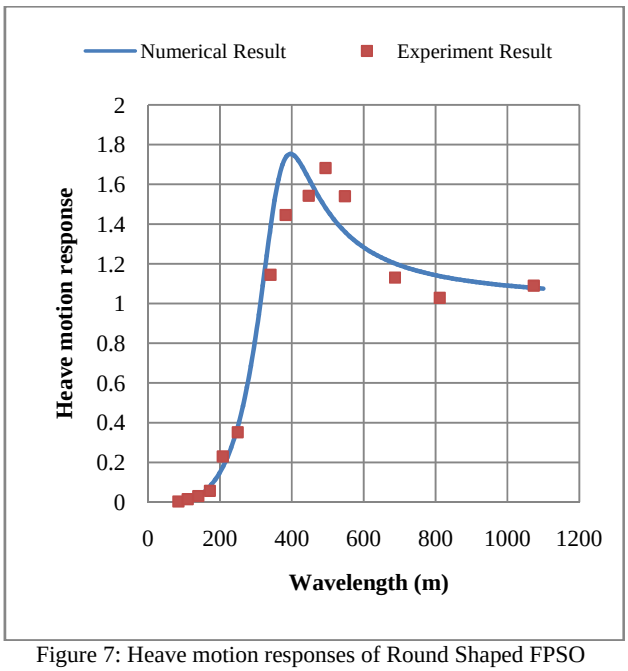

Figure 7: Heave motion responses of Round Shaped FPSO

5.2 Round Shaped FPSO Wave Response

The predicted Round Shaped FPSO wave response characteristic for surge, pitch and heave motion by numerical and experiment method is showed in Figure 5 to Figure 7. In the head sea condition, the surge motion of the Round Shaped FPSO is low for short wavelength region. From the Figure 5, it is showed that the surge RAO which correspond to wave height is below 1.0 for the wavelength less than 980 meters. The relative low surge RAO is important for the offloading operation. This is because lower motion in horizontal plan can help in reducingpossibility of crash between FPSO and ship during offloading operation. Besides that, lower horizontal plan motion is important to avoid damage to the riser.

The more important in FPSO design is reduce the motion in the vertical plan motion. The Round Shaped FPSO also showed relative good wave response characteristic in heave and pitch response in short wavelength region. The FPSO design normally is depend on it operating environment condition. As example, let consider the normal operational of the FPSO in wind seas is between 2 to 7 seconds (wavelength 6 ~76 meter) and ocean swells condition of 12 to 18 seconds (wavelength 225 ~506 meter) (Example of North West Australia sea condition) [9]. The Round Shaped FPSO has very low pitch and heave motion response in the wind sea condition. However, the designed FPSO is not favor to operate in the swell condition due to the natural heave period is located in between the swell sea wave period for the selected operating environment.

From the study, it is observed that the Round Shaped FPSO model have very low pitch or roll motion even though in swell sea environment. The pitch or roll RAO of the FPSO at wavelength less than 506 meter is below 0.5 Rad.m/m ($Radian \times wavelength/wave\ height$). To able the FPSO operate normally, the roll angle must as low as possible especially for FPSO installed with fractionating columns such as LGP and LNG FPSO. The maximum allowable roll amplitude for this type of FPSO is typically below 2 degrees) [10]. Hence, the low pitch or roll motion of Round Shaped FPSO could be help to reduce the down time in most of the wave condition.

From the simulation and experiment test, it is proved that the Round Shaped FPSO have a good dynamic stability in wave condition. The designed FPSO have the natural heave and pitch period occur at 16.1 seconds and 25.7 seconds respectively. By compared to the environment condition, the natural heave period and natural roll/pitch period of this FPSO success avoided the region where most ocean wave take place. However, the heave motion response of this FPSO should be proper modified for it operating environment so the large heave motion in swell condition can be avoided. In opposite, the natural roll/pitch period is located outside the ocean swells and wind sea periods. This advantage also help the FPSO remain stable in most of wave condition.

6.0 CONCLUSION

The study the wave frequency motion of Round Shaped FPSO is conducted by numerical method and experimental method in this research. Both the numerical and experimental result is agreed between each other for surge, pitch and heave motion of FPSO. The simulation results showed that the Round Shaped FPSO has good wave frequency response and the motion response is kept in low amplitude in most of ocean environment. From the research, it is obtained that the designed Round Shaped FPSO has good dynamic stability where this is an important factor to reduce the down time of FPSO in normal operation. Besides, this FPSO also suitable to operate in more stringent requirement, such as design for a LPG or LNG FPSO installed with the fractionating columns. It is believed that maximum roll amplitude of the Round Shaped FPSO can be remain below 2 degrees for most of the wave condition due to low roll or pitch RAO in wind sea and swells sea condition and the roll/pitch natural period is designed far away from the most frequent occur ocean condition. In future, the Round Shaped FPSO design should be focused in heave motion response due to the heave natural period is still possible to fall in the ocean swells condition at some of the FPSO operating environment. From the research, the Round Shaped FPSO can be considered as an alternative to replace ship hull FPSO due to the good wave motion response characteristic and good stability in wave.

ACKNOWLEGMENT

The authors are very grateful to Faculty of Mechanical Engineering, Universiti Teknologi Malaysia, Ocean and Aerospace Research Institute, Indonesia, Department of Transportation and Environmental Systems, Hiroshima University, Japan, National Research Institute of Fisheries Engineering (NRIFE), Japan and Centre for Marine Technology and Engineering (CENTEC), Instituto Superior Técnico, Universidade de Lisboa, Portugal for supporting this research.

REFERENCE

1. Lamport, W. B. and Josefsson, P.M.(2008). The Next Generation Of Round Fit-For-Purpose Hull Form FPSOS Offers Advantages Over Traditional Ship-Shaped Hull Forms,*2008 Deep Gulf Conference*, December 9-11, New Orleans, Louisiana, USA.
2. Arslan, T., Pettersen, B. and Andersson, H.I. (2011). *Calculation of the Flow Around Two Interacting Ships*, Computational Methods in Marine Engineering IV, L.Eça, E. Oñate, J. García, T. Kvamsdal and P. Bergan (Eds.), pp. 254-265.
3. Afrizal, E., Mufti, F.M., Siow, C.L. &Jaswar. (2013). Study of Fluid Flow Characteristic around Rounded-Shape FPSO Using RANS Method. *The 8th International Conference on Numerical Analysis in Engineering*: 46 – 56. Pekanbaru, Indonesia.
4. Kvittem, M.I., Bachynski, E.E. & Moan, T. (2012). Effect of Hydrodynamic Modelling in Fully Coupled Simulations of a Semi-Submersible Wind Turbine. *Energy Procedia* 24.
5. Koto, J., Siow, C.L., Khairuddin, Afrizal, N.M., Abyn, H., Soares, C.G., (2014). Comparison of Floating Structures Motion Prediction between Diffraction, diffraction-viscous and diffraction-Morison methods. *The 2nd International Conference on Maritime Technology and Engineering*. Lisboa, Portugal.
6. Siow, C.L., Koto, J, Yasukawa, H., Matsuda, A., Terada, D., Soares, C.G., Zameri, M. (2014). Experiment Study on Hydrodynamics Characteristic of Rounded- Shape FPSO, *The 1st Conference on Ocean, Mechanical and Aerospace-Science and Engineering-*.Pekanbaru, Indonesia.
7. Siow, C. L., Koto, J, and Khairuddin, N.M. (2014). *Study on Model Scale Rounded-Shape FPSO's Mooring Lines*, Journal of Ocean, Mechanical and Aerospace Science and Engineering, Vol. 12.
8. Christina Sjöbris, (2012). Decommissioning of SPM buoy, *Master of Science Thesis*, Chalmers University of Technology, Gothenburg, Sweden.
9. Jinzhu Xia. (2012). FPSO Design to Minimise Operational Downtime due to Adverse Metocean Conditions off North West Australia. *Deep Offshore Technology*.Perth, Australia
10. Khaw T., Rawstron P. and Lagstrom K., (2005), A New Approach to the Design of Monohull FPSOs, *24th International Conference on Offshore Mechanics and arctic Engineering*, Halkidiki, Greece.